SIMULATION STUDY ON LANDING BEHAVIOR OF SPACECRAFT IN MICROGRAVITY ENVIRONMENT BASED ON MULTIBODY DYNAMICS MODEL

Haruhi Katsumata[1], Genya Ishigami[2]

[1]*Department of Mechanical Engineering, Keio University, Japan, E-mail: haruhi_katsumata@keio.jp*

[2]*Department of Mechanical Engineering, Keio University, Japan, E-mail: ishigami@mech.keio.ac.jp*

ABSTRACT

This paper presents a dynamic simulation of a spacecraft landing in microgravity environment. The landing behavior of the spacecraft in microgravity may be different from that in nominal planetary body such as the Moon or the Mars. This is because the fact that unstable components of the spacecraft such as fuel or solar array paddles will excite additional vibration of the spacecraft. Therefore, this paper addresses a comprehensive mechanical model of a spacecraft and simulates a dynamic behavior of the spacecraft in the landing phase. The model elaborated in this paper typically focuses on two mechanical components: the solar array paddles composed of flexible structure and the sloshing phenomena of the fuel. The model also examines an interaction of the landing gear. The simulation study based on the mechanical model is performed under different slope angles and fuel masses. The result evaluates the landing behavior using metrics in terms of the displacement and orientation of the spacecraft.

1 INTRODUCTION

It has been widely well known that the minor body may provide important clues for the origin and subsequent evolution of the solar system. Several minor body exploration missions have been performed: a giant leap for the minor body exploration was achieved by the Hayabusa mission [1] in which the spacecraft collected samples from the surface terrain and brought them back to the Earth.

A critical scenario in the minor body exploration is a landing phase of the spacecraft. The landing sequence should be autonomously executed since the communication latency due to the distance from the Earth to a minor body is tremendously long. Therefore, an autonomous system for the landing sequence is necessary which can accurately detect any obstacles and avoid potential hazards. Especially, a collision of any parts of the spacecraft other than the landing pads will lead a fatal damage to the spacecraft, resulting its mission failure. Therefore, in order to avoid such a trouble, it is indispensable to access the autonomous system and to analyze the landing behavior of the spacecraft in advance. Since the gravity of an asteroid is much smaller than that of the Earth, an experimental approach for the landing analysis on the Earth may not be reliable, therefore, dynamic simulation is suitable for the landing behavior analysis of a spacecraft. [2]

While landing technology for the planetary bodies such as the Moon or the Mars have been well developed and demonstrated [3][4], there are few cases in which landing analyses and demonstrations in microgravity environment have been performed. Kubota et al. investigated a landing behavior of the Hayabusa on the Itokawa landing sequence [5]. The dynamics model in its work especially focused on the main body and legs, however, other mechanical components such as the Solar Array Paddles (SAP) may excite additional vibration for the main body. In addition, the liquid fuel in the tank may slosh under the microgravity environment that leads external force to the body [6][7]. Therefore, for an accurate analysis of the landing behavior, these components should be thoroughly taken into account.

This paper therefore addresses a comprehensive dynamics model of the spacecraft that considers the SAP model as well as fuel sloshing mechanism in microgravity. The multibody dynamic simulation based on the model is then performed. The simulation result for the landing behavior reveals the landing stability with regard to slope angle and fuel mass.

The rest of this paper is organized as follows: Section 2 introduces the mechanical model developed in this work. Here, this work refers to a spacecraft which will be launched in the mission called *Martian Moons eXploration* by JAXA [8]. Section 3 describes the simulation results and discussions on the landing stability. Section 4 shortly summarizes the work and notes the future prospect of this work.

2 MECHANICAL MODEL

2.1 Multibody Dynamics Model

This work assumes that the spacecraft consists of multiple rigid body, each of which is connected by a rotational/translational joints. The equation of motion for the multibody dynamics is written as:

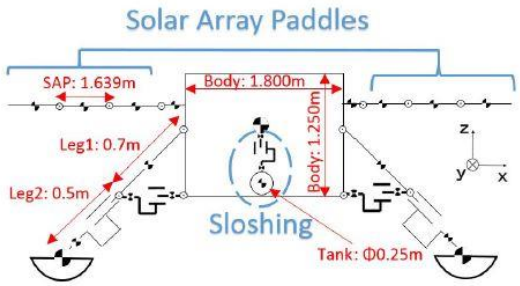

(a): Front view

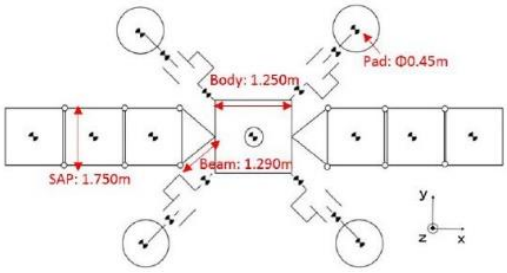

(b)Top view

Figure 1: Articulated multibody dynamics model

$$\boldsymbol{H}\ddot{\boldsymbol{q}} + \boldsymbol{C}(\dot{\boldsymbol{q}}) + \boldsymbol{G} = \boldsymbol{\tau} + \boldsymbol{J}^{\mathrm{T}}\boldsymbol{F} \qquad (1)$$

where $\boldsymbol{H}$ is the inertia matrix of the body, $\boldsymbol{C}$ is the velocity dependent term, $\boldsymbol{G}$ is the gravity term, $\boldsymbol{F}$ is the external forces, $\boldsymbol{\tau}$ is the joint torques, and $\boldsymbol{q}$ is the joint state variables. The schematic illustration of the multibody model of the spacecraft considered in this paper is shown in Figure 1. The model is composed of the main body with the fuel tank, SAPs, and landing gears including landing legs and pads. The specifications of the model are summarized in Table 1 and 2.

Table1: Dynamics parameters for Probe

Link Body	Dimension [m]	Mass [kg]
Main Body	Width: 1.800	700
	Height: 1.750	
	Depth: 1.250	
SAP	Width: 1.639	80
	Height: 1.750	
	Depth: 0.015	
Strut	Width: 1.290	10
	Height: 0.090	
	Depth: 0.050	
Upper Leg	Length: 0.700	30
	Radius: 0.050	
Lower Leg	Length: 0.500	30
	Radius: 0.035	
Pad	Radius: 0.225	10
Fuel Tank	Radius: 0.125	m_{fuel}

Table2: Joint parameters

SAP Joint	Spring	8.0×10^5	[N/◦]
	Damper	4.0×10^3	[N / (◦/s)]
Leg Joint	Spring	50	[N/m]
	Damper	0.3×10^3	[N / (m/s)]
Sub-strut Joint	Spring	1.0×10^3	[N/m]
	Damper	1.3×10^3	[N / (◦/s)]
Sloshing Model	Spring	10	[N/m]
	Damper	$3\sqrt{10 \times m_{fuel}}$	[N / (m/s)]
Terrain model	Spring	1.5×10^3	[N/m]
	Damper	4.4×10^3	[N / (m/s)]

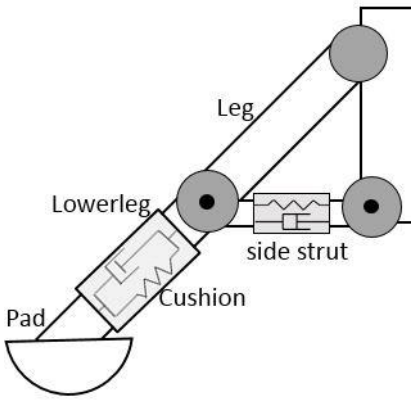

(a) Detail of the leg model

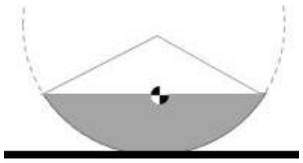

(b) Detail of the pad model

Figure 2: Detail of the landing gear model

2.2 Leg Model with Honeycomb Structure

In this study, the leg model is assumed to be a honeycomb core as a shock absorbing material (Figure 2(a)) to mitigate the impact of landing [9]. The probe has four legs, each of which is evenly allocated on the lower corner of the main body of the probe. The angle between the primary axis of the leg and the body edge is set as 45°.

The leg is composed of the upper leg, lower leg, sub-strut, and pad. Each component is assumed as rigid body and connected via mechanical joints: the main body, the upper leg, and the sub-strut are interconnected via the rotational joints composed of spring-damper system, which perpendicularly intersects the direction of the leg axis.

The honeycomb structure in the lower leg is

modeled as the translational joint that works as the shock absorbing mechanism for the impact of contact force when the probe lands. Also, the sub-strut is also modeled as the translational joint which works as the lateral impact absorption. It should be noted that the honeycomb structure shows three distinctive phases in its force-strain curve. The second phase called Prato Area plays a significant role for the absorption since the strain in this phase increases even while the force applied is constant. These three phases are model by using different spring constants [10].

The landing pad is assumed that its shape is a bottom quarter of the sphere as shown in Figure 2 (b), and the center of gravity of the pad is fixed with the rotational joint via the lower leg.

2.2 SAP Model

The SAPs may have significant influence for the stability of the probe since its flexible characteristics will excite vibration, generating additional external force. In order to simulate such vibration and deflection, the SAP model consists of three rigid thin plates per side with inserting the elastic hinge joint between the adjacent rigid plates (Figure 3). The elasticity is assumed to have characteristics frequency of 100 Hz and a damping factor of 5%. In this way, it is possible to simulate a situation where the SAP vibrates and deflects owing to its inertia or an impact force.

2.3 Sloshing Model

Sloshing is a phenomenon where a fluid passively moves inside its chamber/tank owing to a mechanical vibration of the chamber/tank. Especially in microgravity, this phenomenon becomes significant. We modeled this phenomenon by mechanical components as the well-known approach for the sloshing model with rigid bodies [11].

The liquid fuel in the tank is modeled as the three-dimensionally rotational mass-spring-damper joint (Figure 4). This model uses the ball joint and the linear joint from the tank geometric center, where r is the distance from the tank geometric center to the liquid gravity center, φ is the direction of the center of gravity which freely moves by an external force. This model can simulate the sloshing movement of the whole liquid in the tank, which generates forces or displacement of the center of gravity of the liquid.

2.4 Contact Model to the surface

The contact model between the landing pad and the surface terrain is considered as linear spring-damper system with regard to the pad penetration depth to the terrain (Figure 5). The contact force is calculated as:

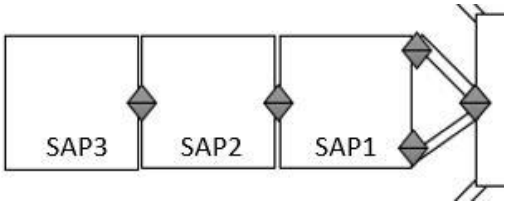

Figure 3: Mechanical model for the SAP

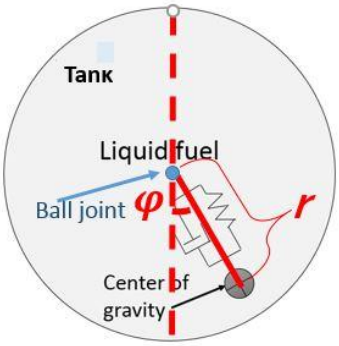

Figure 4: Sloshing model in spherical tank

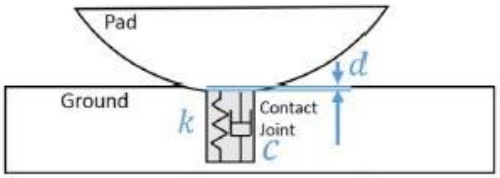

Figure 5: Contact model between the pad and the ground

$$F_{contact} = kd + C\dot{d} \tag{2}$$

where k is the elastic coefficient of the celestial body surface, C is the damping coefficient, and d is the penetration depth of the pad measured from the terrain surface. It should be noted that the terrain parameters of the Martian moon surface are quite uncertain. Therefore, this contact dynamics will be subject to change for more reliable simulation. The friction coefficient in the shearing directions is set as infinity for critical case [3].

3 SIMULATION AND ANALYSIS

The simulation study of the landing behavior of the spacecraft is performed using the dynamics model described in the previous section. In the simulation study, two input parameters, liquid fuel mass and terrain slope angle are considered as uncertain parameters since it is clearly deduced that these two parameters may significantly affect to the landing behavior. For safety evaluation of the landing, the following indices are used: the probe stability in terms of its orientation and displacement.

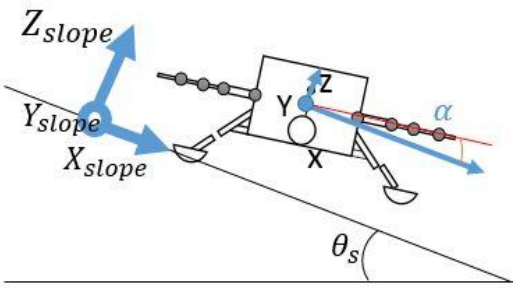

Figure 6: Pitch angle relative to the slope terrain

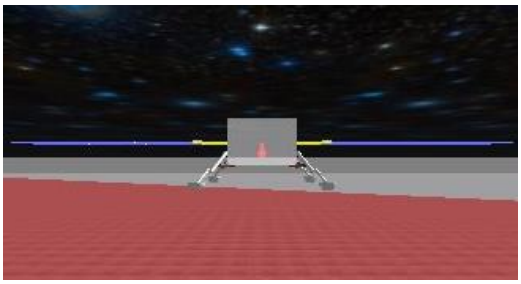

Figure 7: Simulation overview in initial state

3.1 Simulation Condition

In this simulation, the probe is assumed to land on flat sloped terrain having an angle of θ_s [°] (Figure 6). The right-handed coordinate fixed on the slope shown in this figure is defined such that the x-axis is aligned with the slope downhill direction. Here, we introduce a metric defined as α [°] which measures the pitch angle of the probe in the slope coordinate. α is calculated as follows:

$$\alpha = \theta_{pitch} - \theta_s \quad (3)$$

where θ_{pitch} is the pitch angle of the probe in the inertia coordinate. α can be used as the stability index of the probe relative to the terrain slope: the positive α means the probe rotates to the slope downhill while the negative α indicates the probe rotates to the slope uphill direction.

The dynamic parameters of the probe has been already summarized in Table 1. The input uncertain parameters for the fuel masses are set as m=250 kg, 800 kg, and 1200 kg (minimum, nominal, and maximum cases). The slope angle θ_s is set from 0.0° to 9.0 with a step of 1.0, and the slope angle of 4.5° is also tested because the SAP contact occurs around this angle.

The probe in the simulation starts its free fall from the height of 4.0 m in the inertia coordinate with zero pitch angle. Then the probe contacts its pad(s) at the height around 2.0 m. The gravitational acceleration in the simulation is set as 1/1700 G referring to the Phobos' average gravity acceleration.

The simulation was performed from the simulation time t = 0 s to t = 900 s with the time step of 0.1 milliseconds. The probe stability is evaluated from the state valuables calculated from 600 s to 900 s since the probe is required to be stable at 600 s and to maintain it 300 s.

The overview of the simulation (θ_s=5◦, m= 800 kg, t=0 s) is indicated in Figure 7. The center box models the main body of the probe (thrusters, antennas, and other external components are not illustrated); the red sphere inside the box is the center of gravity of the sloshing model pendulum; the yellow box is the beam which connects the main body and the SAP; and the blue boxes are the SAP. The slope is indicated by the translucent red plate under the probe model. When the probe contacts to the slope with the pad(s), the gray marker(s) appear in the simulation drawing while the dark blue marker appears when other components contact.

3.1.1 Definition of the SAP Contact

The SAP protrudes from the main body as shown in Figure 7 so that it may easily touch with the terrain and the contact of the SAP should be carefully detected in the first. Therefore, the contact detection sensor inserted on the tips of the either SAP model. The simulation run terminates once the either sensor detects its contact. There are three conditions of the SAP contacts, downhill-contact, uphill-contact, and no-contact. The contact condition and its timing changes as the input uncertain parameters.

In Figure 8, the downhill contact and the uphill contact are indicated. It can be said that the downhill contact occurs because the SAP is deflected and the whole probe rotates in its pitch axis. The uphill contact occurs owing to the geometric limit determined by the SAP length. In this case, the uphill contact appears before the pad contacts.

3.1.2 Definition of Probe Instability

Once the probe lands on the slope with no contact of the SAP, the probe may be still subject to instable behavior. Such instability is composed of two metrics: one is the tipping over of the probe and the

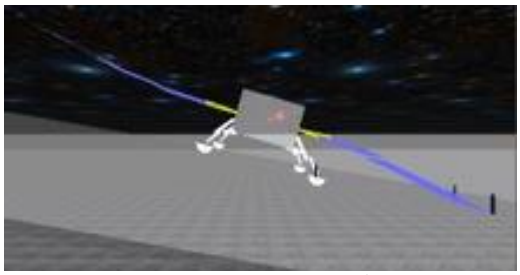

(a) Downhill contact case of the SAP

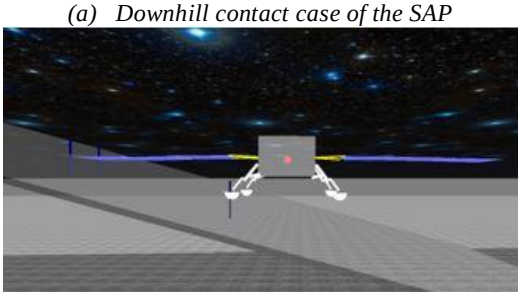

(b) Uphill contact case of the SAP

Figure 8: SAP contact cases

other is the residual vibration of the main body. The tipping over indicates a risk of overturning of the probe or crashing the SAP. The residual vibration means that the probe maintains its shaking even after the landing. Larger values for these metrics make the landing or sampling difficult.

For analyzing these stability metrics of the probe, the time series data of the relative pitch angle α is used. This is because that landing on the sloped terrain as already shown in Figure 7 and 8 easily let the probe rotate owing to the slope angle. The tipping over risk α_{ave} is calculated as an average of the time series data of α between the periods from t =600 s to t= 900 s, and the residual vibration α_{std} is defined as a standard deviation of α in the same periods.

3.1.3 Definition of a Displacement

The probe potentially moves or slides considerably in the horizontal direction while it lands on slope terrain. When the terrain is soft, or the particle of regolith is small, such sliding motion is easy to occur. The displacement is critical because larger displacement increases additional risks in tipping over, damages in the lading gears, or collision to rocks. Therefore, in this study, the allowable displacement of the probe is set less than 10 m. The displacement value means the amount of distance from the first touch point to the center of the probe at t = 600 s.

3.2 Simulation Results

3.2.1 Discussion on the SAP Contact

Table 3 summarizes SAP contact conditions in varied slope angles with different liquid fuel masses: m=250, 800, and 1200 kg.

In Table 3 and Figure 8, the geometric limit due to the probe configuration is obvious: in any liquid fuel masses, the uphill contact occurs over the slope angle of 9.0°. The downhill contact occurs in different slope angles with regard to the fuel masses. The downhill contact is categorized in two situations as shown in Figure 9 and 10: the contact may be due to the SAP deflection and/or the rotation of the body. It should be noted that the safe landing are seen in the range of $4.5° < \theta_s < 8°$ for the case of m = 800 kg, and $5° < \theta_s < 9°$ for m = 1200 kg. In these slope angles, the SAP never contact with the ground: the SAP deflection and the body rotation may not be remarkable because the landing impact may be somewhat absorbed by the leg or the rotational moment of the body around the pitch may be small in these cases.

Additional simulation study in which the stiffness of the SAP is doubled ensures the abovementioned results. For the stiffer SAP, the downhill contact of the SAP never occur in the case of m=800 or 1200 kg. The downhill contact still occur in the range of $4° \leq \theta_s < 8°$ when m=250 kg. These results indicate that the stiffer SAP is favorable, in particular when the liquid fuel mass is so small.

Table 3: SAP contact cases in different fuel mass

	Liquid fuel mass m[kg]		
Contact case	250	800	1200
uphill	$9° \leq \theta_s$	$9° \leq \theta_s$	$9° <= \theta_s$
downhill	$6° \leq \theta_s < 9°$	$4° \leq \theta_s < 4.5°$	$4° < \theta_s \leq 5°$
		$8° \leq \theta_s$	

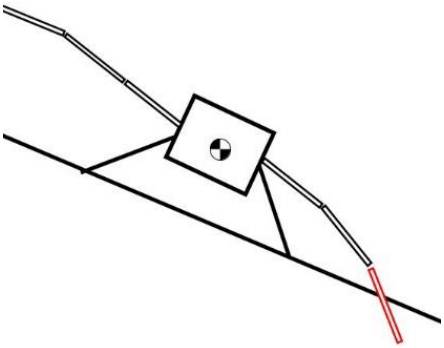

Figure 9: Downhill contact by the SAP deflection

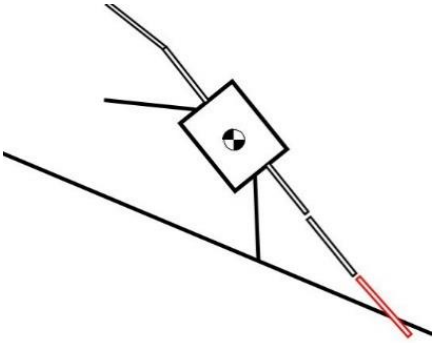

Figure 10: Downhill contact by the whole rotation

3.2.2 Discussion on Probe Stability

The stability of the probe with the liquid fuel mass of m=250 kg, 500 kg, and 1000 kg is also analyzed. The slope angle varies from 0.0° to 4.0° with a step of 0.1°. Figure 11 shows the trend of the pitch angle of the probe relative to the slope. Some peaks of the pitch angle when m = 250 and 500 kg can be seen at the points where the slope angle are 1°, 2° and, 3°. These peaks may be deduced that the flexible components including the SAP and sloshing fuel may resonate one another and absorbs the moment around the pitch axis of the body. On the other hand, for m=1000 kg, there is no peak for the pitch angle in any slope angle. Therefore, it can be said that heavier liquid fuel mass will make the probe stable because the fuel would not move remarkably generating less additional external momentum.

Figure 11 also indicates that the pitch angle takes negative values in the most cases. Such situation is depicted in Figure 12, where the pads on the uphill side may stick to the ground and the probe may not tend to turnover. The positive pitch angle shown in Figure 13 is also found in some cases. These

distinctive cases are also due to the force vector of the contact dynamics. The rotational direction of the probe highly depends on the geometric relationship between the center of gravity of the main body and the coupled force vector generated at the contact patch.

The residual vibration measured by α_{std} is less than 0.25° in any cases. This is not critical and the dynamic stability is found to be little problem in this model.

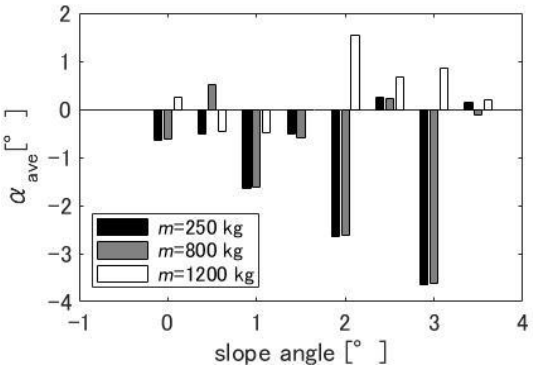

Figure 11: Pitch angle at stable time under different slope angles

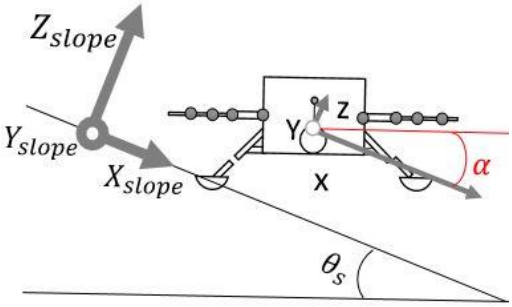

Figure 12: Negative pitch angle

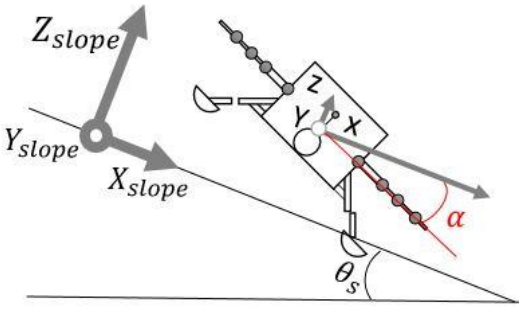

Figure 13: Positive pitch angle

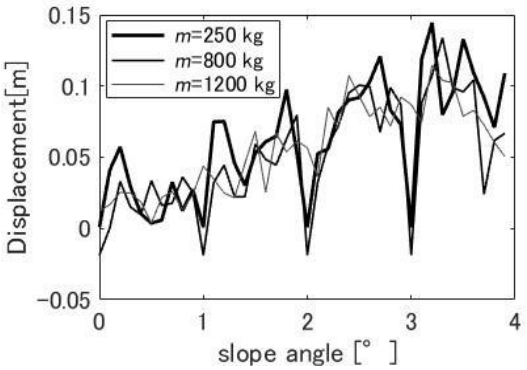

Figure 14: Displacement of the probe

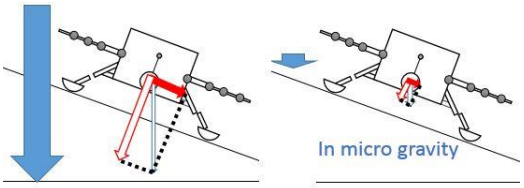

Figure 15: Influence of gravitational acceleration

3.2.3 Discussion on Probe Displacement

The displacement of the probe is shown in Figure 14. The displacement is within 0.15 m in any cases. This is not critical because the critical limit is set as 10 m. So, in this time, the displacement is found to be little problem in this model. On the other hand, in this study, the frictional force is set infinite so that the probe hardly slides in lateral direction but it horizontally hopped, but not remarkable. As seen in Figure 15, the tangential component of the gravitational pull in the microgravity environment is much smaller than that on the Earth, and therefore the displacement is so small.

4 CONCLUSION

This study has focused on the development of the mechanical model of the landing probe in the microgravity environment. The model considered in the paper has included the sloshing of the liquid fuel as well as the SAP flexibility and the complicated design of the landing gear.

The simulation study of the multibody model in micro-gravity has revealed that heavier liquid fuel mass is preferable for stable landing since the sloshing works as absorbing mechanism in the landing phase. In addition, the influence of the resonance between the mechanical components significantly characterizes the microgravity landing. In particular, the SAP stiffness is quite important issue for safe landing since the SAP flexibility may make the SAP touch on the terrain surface.

References

[1] Hajime Mita (2015), Origins of Life and the Studies of Organic Analyses in Cosmic Samples, Journal of the Surface Finishing Society of

Japan, 66(9): pp. 397-402, (in Japanese).
[2] Yoji Umetani, Kazuya Yoshida (1989), Resolved Motion Rate Control of Space Robotic Manipulators with Generalized Jacobian Matrix, Journal of The Robotics Society of Japan,7 (4): pp. 327-337, (in Japanese).
[3] Masahiro Nohmi and Akira Miyahara (2005), Modeling for Lunar Lander by Mechanical Dynamics Software, *Proc. of the 2005 AIAA Modeling and Simulation Technologies Conference and Exhibit*, San Francisco, California, pp.1-8.
[4] Douglas S. Adams (2008), Phoenix Mars Scout LConanding Risk Assessment, *Proc. of the 2008 IEEE Aerospace Conference Robotics and Automation*, Big Sky, MT, USA, pp. 1095-323X.
[5] Takashi Kubota, Masatsugu Otsuki, Tatsuaki Hashimoto (2008), Touchdown dynamics for sample collection in Hayabusa mission, *Proc. of the 2008 IEEE International Conference on Robotics and Automation*, Pasadena, CA, USA, 2008, pp.158-163.
[6] Himeno Takehiro (2013), Propellant Management in Liquid Rockets and Space Vehicles, Japanese Journal Of Multiphase Flow 27(4), pp.385-392,m (in Japanese).
[7] Keiji Komatsu (2015), *sloshing*, MORIKITA PUBLISHING Co., (in Japanese).
[8] JAXA. Martian Moons eXploration. http://mmx.isas.jaxa.jp/index.html (as of April 2018).
[9] Kazuya Yoshida, Yoichi Nishimaki, Hiroshi Kawabe, Takashi Kubota (2002), Analysis Of Touch-Down Dynamics and Sampling Sequence Of Muses-C, *34th COSPAR Scientic Assembly /2nd World Space Congress*, Houston, TX, USA.
[10] Masahiro Nishida, Koji Teranishi, Effects of Specified Filled Cell Patterns on In-plane Dynamic Compressive Properties of Aluminum Honeycombs, Journal of the Japanese Society for Experimental Mechanics,13(3), pp.257-263, (in Japanese).
[11] Miao Nan, Li Junfeng, Wang Tiansh (2016), Large-Amplitude Sloshing Analysis and Equivalent Mechanical Modeling in Spherical Tanks of Spacecraft, Journal of Spacecraft and Rockets, 53(3), pp. 500-506.